Susceptibility Screening of Winterberry Cultivars Against Latent Fruit Rot, and Identification of Metabolites Correlated with Rot-resistant Phenotypes[1]

Isabel B. Emanuel[2], Jessica L. Cooperstone[3,4], and Francesca Peduto Hand[2]*

Abstract

Winterberry [*Ilex verticillata* (L.) A. Gray] is a species of deciduous holly bearing colorful fruit, and is popularly used in landscape design and as specialty woody cuts for fall and winter seasonal decoration. Latent fruit rot of winterberry, caused by the fungus *Diaporthe ilicicola*, has recently afflicted nurseries in the Northeastern and Midwestern United States. Trials conducted in 2021 and 2022 screened eight commercially available winterberry cultivars for their susceptibility to the disease. Results showed that not all cultivars are equally susceptible, and that 'Maryland Beauty' and 'Winter Red' consistently had the lowest disease ratings. UHPLC-MS/MS metabolomic analysis was used to determine whether differences in susceptibility are reflected in the fruit metabolome. Principal components analysis of whole metabolome data showed a distinct separation of the less susceptible cultivars from the more susceptible cultivars, and univariate analysis comparing these two groups of cultivars at three phenological timepoints (corresponding with fruit set, fruit color change, and fruit maturation) found 89 features present at a significantly higher relative abundance in the less susceptible cultivars. Some compounds identified in less susceptible cultivars with reported antifungal bioactivity are derivatives of terpenes, cinnamic acids, and stilbenes. These results suggest that differences in susceptibility could be based on the presence of antifungal compounds within winterberry fruit. Future research to further identify unknown features and assess compound bioactivity against winterberry fruit rot pathogens should be done to inform both resistance breeding efforts and chemical or biological control programs.

Species used in this study: Common winterberry [*Ilex verticillata* (L.) A. Gray]; *Diaporthe ilicicola* S. Lin, Taylor & Peduto Hand, 2018.

Index words: antifungal compounds, cultivar resistance, fruit metabolomics, *Diaporthe iliciola*.

Significance to the Horticulture Industry

Common winterberry is a deciduous shrub, bearing red, orange, or yellow fruit that persist on the plants through fall and winter. In the U.S., wholesales of winterberry woody cuts have an annual revenue of $1.5 million (NASS 2019) and allow for an extension of the growing season in many nurseries. Latent fruit rot of winterberry, caused by the fungus *Diaporthe ilicicola,* has been confirmed in nurseries throughout the Northeastern and Midwestern U.S., with up to 100% crop loss reported. This study aimed to determine whether resistant phenotypes exist within commercially available winterberry cultivars to provide nursery growers with recommendations when establishing new plantings. Eight cultivars were assessed including: 'Winter Red', 'Winter Gold', 'Chrysocarpa', 'Roberta Case', 'Maryland Beauty', 'Red Sprite', 'Magical Showtime', and 'Stoplight'. Cultivars Winter Red and Maryland Beauty were found to develop lower levels of disease under both natural and artificial inoculum conditions, and in both field and container yard production systems; therefore, these cultivars should be preferred over others in nurseries with a history of the disease. Metabolic analysis of the eight winterberry cultivars screened for susceptibility in the field showed that the fruit of less susceptible cultivars display distinctly different metabolic profiles compared to the more susceptible cultivars. Eighty-nine metabolite features were identified as being putatively related with the less susceptible phenotype, due to their increased presence in less susceptible cultivars compared to more susceptible cultivars. Future work will determine the compound identity of these features of interest and determine which are bioactive against *D. ilicicola*.

Received for publication March 9, 2023; in revised form May 4, 2023.

[1]This research was supported by a grant from the Horticultural Research Institute ("HRI"). Its contents are solely the responsibility of the authors and do not necessarily represent the views of HRI. This work was also supported in part by USDA-NIFA Education and Workforce Development Predoctoral Fellowship grant No. OHO03082-CG/project accession no. 1026587, and USDA-NIFA Hatch Project No. 1020446. Any opinions, findings, conclusions, or recommendations expressed in this publication are those of the authors and do not necessarily reflect the view of the U.S. Department of Agriculture. The research described in this paper represents a portion of the dissertation submitted by I. B. Emanuel to the Office of Graduate Studies of The Ohio State University to partially fulfill requirements for the PhD degree in Plant Pathology. The authors would like to thank members of the Ornamental Crops Pathology Lab at The Ohio State University, as well as staff members at the Kottman Greenhouses and Waterman Agricultural and Natural Resources Laboratory Complex, for assistance conducting outdoor trials. We would also like to thank S. Ghosh and J. L. Hartman for their advisement regarding metabolomic analysis, and our commercial nursery partner for allowing us to conduct outdoor trials in their facility for a portion of this work.

[2]Department of Plant Pathology, The Ohio State University, Columbus, OH 43210, USA.

[3]Department of Food Science and Technology, The Ohio State University, Columbus, OH, 43210, USA.

[4]Department of Horticulture and Crop Science, The Ohio State University, Columbus, OH, 43210, USA.

*Corresponding author email: hand.81@osu.edu.

Introduction

The genus *Ilex* (commonly referred to as holly) includes over 600 species of woody perennial trees, shrubs, and climbing vines with both deciduous and evergreen foliage (Galle 1997). The genus has a near-global distribution,

with the cultivation of select species for their culinary, medicinal, and ornamental value, stemming from several distinct origins in Europe, Eastern-Asia, and South America (Deng et al. 2015, Dengler 1957, Alikaridis 1987, Galle 1997). While the fruit of *Ilex* are mildly toxic for human consumption, the leaves, stems and roots of many species are known to contain high levels of bioactive metabolite classes, including triterpenoids, saponins, purine alkaloids, and phenolics; because of these constituents, they are popularly used to create stimulating teas and medicinal tinctures (Smith 2019, Hale 1991, Alikaridis 1987). The most well researched *Ilex* metabolome is that of *I. paraguariensis* A. St.-Hil. The leaves and bark of this plant are used to create yerba mate, a popular South American tea, because they contain purine alkaloid stimulants, caffeine and theobromine (Alkaridis 1987). Additionally, the leaves and woody tissue of *I. cassine* L. var. *cassine* (dahoon holly), *I. vomitoria* Ait. (youpon holly), *I. hainanensis* Merr., *I. pubescens* Hook. & Arn., *I. stewardii* S. Y. Hu., *I. guayusa* Loes. (guayusa) are traditionally used to soothe ailments, including indigestion, inflammation, hypertension, cardiovascular disease, non-alcoholic fatty liver disease, and low fertility (Kothiyal et al. 2012, Li et al. 2006, Yang et al. 2018, Duenas 2016).

Ilex verticillata (L.) A. Gray (common winterberry) is among the *Ilex* species well-known for their ornamental value; other popular ornamental species include *I. cornuta* Lindl. & Paxton (Chinese holly), *I. aquifolium* L. (English holly), *I. opaca* Aiton (American holly) and *I. serrata* Thunb. (Japanese winterberry). Winterberry species are deciduous, but their colorful fruits remain on branches throughout the winter, making these plants popular for use in landscape design and as specialty cuts for fall and winter holiday decorations. The total annual wholesale value of *I. verticillata* (L.) A. Gray woody cuts in the United States has tripled over the past several years, increasing from $500K in 2014, to $1.5M in 2019 (NASS 2014, NASS 2019). In 2018, a latent fruit rot disease, caused by the fungal pathogen *Diaporthe ilicicola,* was discovered and has since been resulting in up to 100% crop loss in nurseries throughout the Northeastern and Midwestern United States (Lin et al. 2018). Common symptoms of the disease include early plant defoliation, undersized and shriveled fruit, and fruit rot (Lin et al. 2018). The biology of *D. ilicicola* has been studied, and both environmental and fruit physiological factors putatively associated with symptom development have been identified. These factors include increased light intensity on fruit following plant defoliation, and the presence of biologically active, semi-polar metabolites within the fruit, which may fluctuate in concentration within the fruit during maturation (Emanuel et al. 2023). In these studies, exposure of *D. ilicicola* to winterberry fruit ethanolic extracts, *ex vivo,* resulted in increased pycnidia formation and hyphal melanization (Emanuel et al. 2023). In several fungal systems, pycnidia formation is stimulated by abiotic stress, including increased light exposure and hyphal abrasion (Vasconcelos et al. 2001, Onesirosan et al. 1975). Therefore, it is reasonable to hypothesize that the ability of the ethanolic extracts of winterberry fruit to induce pycnidia formation and hyphal melanization in *D. ilicicola* may suggest that extracts create a stressful environment, possibly due to the presence of antifungal compounds within the fruit. The formation of pycnidia is hypothesized to be involved in symptom development in this disease, as microscopic observation revealed that the formation of *D. ilicicola* pycnidia within the epicarp of winterberry fruit resulted in tears in the fruit cuticle, which facilitated rapid colonization by opportunistic pathogens and consequent fruit rot (Emanuel et al. 2023).

Within *Ilex*, chemical defense utilization against biotic stressors, such as pathogens, varies by species, environmental factors, and type of stressors (Gargiullo and Stiles 1991). Extracts from the leaves, woody tissue, and fruit of many *Ilex* species show inhibition against bacteria, fungi, viruses, and insect pests (Chen et al. 2011, Kothiyal et al. 2012, Wu et al. 2007, Erdemoglu et al. 2009). Of the compounds identified within *Ilex* species, triterpene saponins and polyphenolic acids are the most frequently associated with antimicrobial capabilities. Triterpenes are 30-carbon, non-polar, polycyclic molecules which make up a large class of plant secondary metabolites and often serve as building blocks for plant defense-related compounds (Thimmapa et al. 2014). Triterpenes and triterpene saponins have been reported in the bark, root, fruit and leaf extracts of many *Ilex* species including *I. cornuta*, *I. urceolatus*, *I. paraguariensis* A. St.-Hil., *I. hainanensis* Merr., *I. stewardii* S. Y. Hu., *I. pubescens* Hook. & Arn., and *I. oblonga* C. J. Tseng, all of which have shown to express some level of antifungal, antibacterial, or antiviral ability (Li et al. 2006, Murakami et al. 2013, Chen et al. 2011, Thimmapa et al. 2014, Marakami et al. 2013, Erdemoglu et al. 2009, Wu et al. 2007). Phenolic compounds are another class of compounds commonly utilized in plant defense (Palo & Robbins 1991). Antimicrobial phenolics reported in *Ilex* tissues include several compounds downstream of the phenylalanine deamination pathway, such as chlorogenic acids, tannins, cinnamic acid esters, and flavonoids (Campa et al. 2008). Induced changes in fruit phenolic content have been observed in *I. opaca* Aiton to combat the insect pest, holly berry midge [*Asphondylia ilicicola*] (Gargiullo & Stiles 1991). However, no sign of induced changes in total phenolic content was observed in *I. verticillata* (L.) A. Gray × *I. serrata* Thunb. 'Sparkleberry' fruits in response to a *Diaporthe ilicicola* infection (Emanuel, Cooperstone, and Peduto Hand, personal communication).

The diversity of the *Ilex* genus no doubt contributes to the chemodiversity seen within the bark, leaves, roots, and fruits of these plants. While the chemical constituents of several *Ilex* species, including *I. paraguariensis* A. St.-Hil., *I. vomitoria* Ait., *I. cornuta*, and *I. aquifolium* L. have been explored, the metabolic diversity of deciduous holly species, including *I. verticillata* (L.) A. Gray, remain largely unknown. This study aimed to determine whether commercially available *I. verticillata* (L.) A. Gray cultivars differ in their susceptibility to latent fruit rot caused by the fungus *D. ilicicola*, and whether the resistant phenotype is related to the fruit chemical profile. Results are meant to

aid nursery growers in cultivar selection, and to direct future research towards antifungal compounds within *I. verticillata* (L.) A. Gray fruit which may contribute to disease resistance.

Materials and Methods

Cultivar susceptibility screening – artificial inoculum. An outdoor container trial was conducted at the Waterman Agricultural and Natural Resources Laboratory in Columbus, OH over two consecutive seasons (2021 and 2022) from April through November. Trials used *I. verticillata* (L.) A. Gray female cultivars Winter Red, Winter Gold, Red Sprite, Spotlight, Maryland Beauty, Chrysocarpa, Roberta Case and Magical Showtime, and male cultivars Jim Dandy, Apollo, Southern Gentleman, and Raritan Chief. Male pollinators were selected to ensure flowering overlap with all female cultivars (Resch 2020). Between seasons, plants were overwintered in a covered hoop house near the trial location. All plants were maintained in 28.4 L (7.5 gal) nursery containers filled with COM-TIL bulk compost (Kurtz Bros Mulch & Soils, Central Ohio LLC), and fertilized once at the beginning of each season with 28 g (1 oz) Osmocote® Plus 15-9-12 5-6M slow-release fertilizer (ICL Specialty Fertilizers) mixed into the soil topcoat. Plants were arranged in a randomized complete block design with 4 blocks in a 12.8 m by 14.6 m (45 ft × 48 ft) container yard lined with landscape fabric. In each block, 1-10 plants of each female cultivar constituted a single experimental unit. Although the number of plants in each experimental unit varied, sampling was done randomly from across all plants within each experimental unit. One male per every ten female plants was placed in a row at the center of the field plot, ensuring that all female cultivars were within 161 m (0.1 mile) of a male plant (Galle 1997). Additionally, a bee box was placed in the corner of the plot to facilitate pollination. Plants were watered for 20 min three times daily from May through October using an automated drip irrigation system utilizing 13.6 L per hour (3.6 gph) flow rate emitters. Each season, flowering started in late May and continued through mid-June, depending on the cultivar. At full bloom, which occurred approximately 5-7 days following bloom onset, pots were moved from the trial area and all open flowers and surrounding foliage on each plant were inoculated by spraying a conidial suspension of *Diaporthe ilicicola* (isolate FPH2015-598) at a concentration of 10^5 spores·mL^{-1} prepared as described by Lin & Peduto Hand (2019a), using a non-compressed hand sprayer until runoff. Prior to inoculation, *D. ilicicola* (isolate FPH2015-598) was grown on potato dextrose agar at room temperature 23 C (73.4 F) under fluorescent light (2,700-4,400 lux) with a 14-h photoperiod for 3 weeks to induce sporulation. Following inoculation, plants were covered with a clear plastic sheet in groups of nine and maintained in a closed shed overnight. The following morning, plants were uncovered and returned to their field location. Inoculation days varied dependent upon cultivar to coincide with full bloom (Table 1).

Sampling of fruit was conducted at three timepoints throughout each season, which coincided with (i) fruit set, (ii) fruit color change, and (iii) mature fruit. Incidence and severity of fruit rot were assessed on 50 fruits which were randomly collected from each experimental unit at each sampling time point. Collected fruit were stored on ice or at 4 C (39 F) for no more than 48 h prior to assessment. Disease incidence was expressed as presence or absence of disease symptoms on fruit while disease severity was expressed as the percent of fruit area covered by symptoms. The area under the disease progress curve (AUDPC) was calculated for both disease incidence and disease severity through the three sampling timepoints as described by Madden and Nutter (1995). Cultivars Winter Red and Roberta Case did not have sufficient fruit yield to complete collections in two of the four blocks in 2021; therefore, only two blocks were utilized to calculate disease incidence, severity and AUDPC.

Table 1. Dates in 2021 and 2022 when open flowers of *Ilex verticillata* (L.) A. Gray cultivars were inoculated with a spore suspension of the fungus *Diaporthe ilicicola*. Dates correspond with full bloom (i.e., 5-7 days following the onset of flower bloom).

	Inoculation dates	
***I. verticillata* (L.) A. Gray cultivar**	**2021**	**2022**
Roberta Case	6/1	5/25
Red Sprite	6/1, 6/8[z]	6/1, 6/2[z]
Magical Showtime	6/1	6/1, 6/2[z]
Chrysocarpa	6/8	6/8
Stoplight	6/8, 6/15[z]	6/8
Winter Gold	6/15	6/16
Winter Red	6/15	6/16
Maryland Beauty	6/8	6/16

[z]Plants within select treatments that displayed differential flowering times were inoculated on two different dates to ensure they were in full bloom at the time of inoculum application.

Data were subject to ANOVA analysis using a linear model in base R v. 4.0.4 (https://cran.r-project.org/bin/windows/base/old/4.0.4/). To improve homogeneity of variance, disease incidence datasets were arcsine square root transformed prior to analysis and disease severity datasets were square root transformed. All datasets were back transformed for presentation. ANOVA analysis revealed a significant interaction effect between year and cultivar for all datasets; therefore, data from the two years were separated for post-hoc analysis. Means separation was conducted using Tukey's HSD test (α=0.05).

Cultivar susceptibility screening – natural inoculum. In 2021, cultivar susceptibility trials were conducted at two locations, a field and a container yard, within a commercial nursery in Lake County, OH that had a history of latent fruit rot. Plants in the container yard location were maintained in 19 L (5 gal) nursery pots and the surfaces of the pots were topped with pine needle mulch. At each location, a split-plot trial design was used with the main-plot factor being the cultivar evaluated (n=5 at field location, n=6 at container yard), and the sub-plot factor being the block (n=4 at both locations). The field location contained rows of five cultivars: Winter Red, Winter Gold, Chrysocarpa, Maryland Beauty, and Red Sprite. The container yard had rows of six cultivars: Winter Red, Winter Gold, Chrysocarpa, Maryland Beauty, Red Sprite, and Stoplight. In each block, an experimental unit consisted of a single plant.

Plants at each location were exposed to naturally available inoculum and were not treated with any chemical or subject to any cultural management practices throughout the season. Fruits were sampled from each experimental unit as previously described at three timepoints corresponding to the phenological stages of (i) color change, (ii) mature fruit, and (iii) mature fruit at the end of the season. Collected fruits were assessed for disease incidence and disease severity as previously described. AUDPC was calculated as described by Madden and Nutter (1995) across the three collection timepoints. Cultivar Chrysocarpa in the container yard location did not have sufficient fruit yield to complete collections in three of the four blocks; therefore, only one block was utilized to calculate disease incidence, severity and AUDPC. Additionally, only 35 fruits from the single block were utilized to evaluate disease at the final assessment timepoint at this location.

Data were subject to ANOVA analysis using a split-plot model in R (v. 4.0.4) with the package agricolae (De Mendiburu and Simon 2015) and the function sp.plot(). All datasets were transformed using a natural logarithm prior to analysis and back transformed for presentation. ANOVA revealed differences between the two field locations; thus, data from the two locations were separated for post-hoc analysis. Means separation was conducted using Tukey's HSD test (α=0.05).

Untargeted metabolomic analysis to identify differences in fruit chemistry. Fruit samples were collected from the artificially inoculated plot at the Waterman Agricultural and Natural Resources Laboratory in 2021, to be used for untargeted UHPLC-MS/MS metabolomic analyses to identify differences in fruit chemistry among cultivars. Fruits were collected at three timepoints throughout the season: fruit set (August 31, 2021), color change (September 10, 2021) and mature fruit at the end of the season (November 11, 2021). During collection, 3-5 fruit, up to 2 cm^3, were collected randomly from each experimental unit and placed in a 2 mL microcentrifuge tube. Tubes containing fruit samples were immediately flash-frozen in liquid nitrogen to prevent metabolic changes from occurring. Frozen samples were stored at -80 C until their shipment at the end of the season to the West Coast Metabolomics Center (WCMC, Davis, CA) for untargeted LC-MS/MS analysis.

A semi-polar extraction of fruit samples was done at the WCMC. Protocols were adapted from Fiehn (2006), Salinas & Sanchez-Serrano (2006) and Weckwerth and Fiehn (2004). Briefly, fruit were freeze dried and ground. Twenty mg of fruit powder were weighed out and extracted with 1 mL of cold 80:20 MeOH:H_2O. The slurry was vortexed for 10 sec and centrifuged for 5 min at 14,000 rcf. The supernatant was transferred to a clean 1.5 mL microcentrifuge tube and 450 µL of the liquid samples were aliquoted for analysis. All samples were dried and resuspended in 100 µL 75:25 H_2O:acetonitrile. The resuspension solvent contained six internal standards: 1-cyclohexyl-dodecanoic acid urea (CUDA), D4-Daidzein, D5-Hippuric Acid, 2-[[2-[(2-amino-3-methylbutanoyl)amino]-3-(4-hydroxyphenyl)propanoyl]amino]-3-methylbutanoic acid (Val-Tyr-Val), D3-L-Carnitine, and D9-Reserpine. Samples were vortexed for 10 sec and sonicated for 5 min at room temperature and then centrifuged for 2 min at 16,100 rcf. A method blank sample (containing solvent only) and a quality control sample (consisting of pooled aliquots of test sample extracts) were run every 10 samples for quality assurance. Samples were separated on a Vanquish UHPLC system (ThermoFisher Scientific) equipped with a Thermo Q-Exactive HF Orbitrap MS and an electrospray source, which was operated in both positive (+) and negative (−) modes. The instrument was tuned and calibrated per manufacturer's recommendations. LC-MS/MS data were acquired using the following parameters: mass range 80-1200 *m*/*z*, full scan MS1 mass resolving power at 60,000 with 2 scans of data-dependent MSMS (dd-MSMS) per cycle (4 scans per cycle for pooled MSMS injections), normalized collision energy at 20%, 30%, and 40% with a dd-MSMS mass resolving power at 15,000. Five µL of each sample were injected per run.

Raw spectral data were deconvoluted by the WCMC using MS-DIAL version 4.9. Matrix effects were observed for the internal standard, CUDA, so data were normalized to the sum of identified metabolites. Mass over charge maximum peak heights and retention times were exported for use in statistical analysis. Features with a coefficient of variation greater than 20% in the quality control samples, and greater than 20% average relative abundance in blank samples compared to test samples, were removed from the datasets. Data were imputed in Rstudio (using R v. 4.0.4), and undetected features within samples were replaced with a value corresponding to half of the lowest relative abundance value recorded for that feature across all samples.

Feature clustering was done using the package notame (Klavus et al. 2020) with a connection correlation threshold of 0.95, a retention time window of 1/120, and a clustering threshold of 0.80. Principal components analysis (PCA) was conducted in MetaboAnalyst v. 5.0 (https://www.metaboanalyst.ca/faces/ModuleView.xhtml) to visualize metabolic differences due to cultivar and fruit stage. PCA plots revealed two distinct clustering groups by cultivar and three distinct clustering groups by fruit physiological stage (Fig. 3). Cultivars were separated into two groups based on their clustering by cultivar profile. PC clustering by cultivar included group 1 (denoted as "R"), which contained cultivars Winter Red, Maryland Beauty, and Winter Gold, and group 2 (denoted as "S"), which contained cultivars Roberta Case, Chrysocarpa, Magical Showtime, Stoplight, and Red Sprite. The three collection timepoints were separated for univariate analysis comparing between two PC clustering by cultivar groups (R or S). Significance thresholds for univariate analysis were set such that features were significant if they had a fold change (FC) > 150 and a $P < 0.001$.

Features of interest were identified using the confidence criteria described by Blazenovic et al. (2018). Features annotated to a confidence level of 1, denoting a confident 2D structure with at least two pieces of supporting evidence, were annotated using the MassBank of North America (MoNA) (http://massbank.us/) LC-MS/MS spectral database where data were available. Features annotated to a confidence level of 3, denoting a possible structure or class, were based on a plausible accurate mass match from the

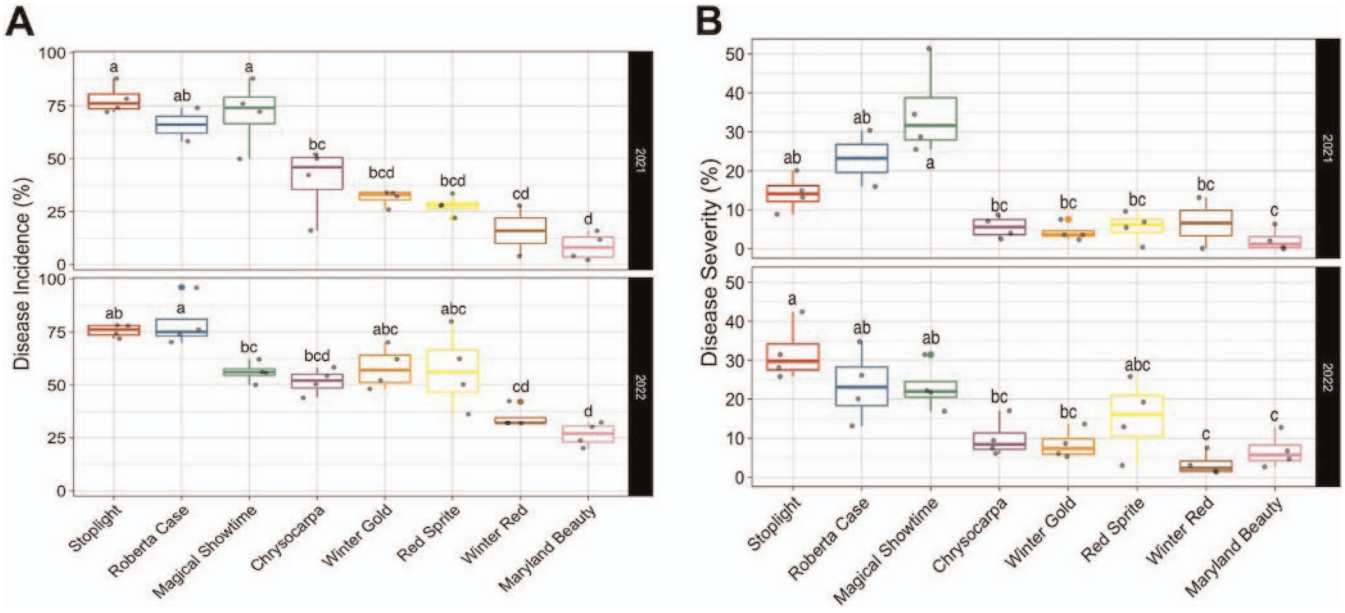

Fig. 1. Mean incidence (A) and severity (B) of latent fruit rot recorded at the end of the 2021 and 2022 growing seasons in outdoor container trials conducted at the Waterman Agricultural and Natural Resources Laboratory in Columbus, OH, with eight commercially available winterberry cultivars artificially inoculated with the fungus *Diaporthe ilicicola* at bloom. The middle line in the boxplot represents the treatment median, while the upper and lower lines represent the upper and lower quartiles. Perpendicular lines connected to the upper and lower quartile lines indicate the range of the upper and lower 25% of datapoints. Datapoints separate from the boxplot indicate outliers. Means separation was performed using Tukey's HSD test (α=0.05). Different letters indicate significant differences in treatment mean.

Human Metabolomic Database (HMDB) (https://hmdb.ca/) v. 5.0. Features which could not be identified using MoNA or HMDB were given an annotation confidence level of 4, denoting an unknown classification.

Results and Discussion

Cultivar susceptibility screening – artificial inoculum. Differences in susceptibility to latent fruit rot were observed between the eight winterberry cultivars tested in both 2021 and 2022 ($P < 0.05$) (Fig. 1). At the end of both growing seasons, the highest levels of disease incidence and severity were consistently observed in the cultivars Stoplight (disease incidence range: 72-88%; disease severity range: 9-42%), Roberta Case (disease incidence range: 58-96%; disease severity range: 13-35%), and Magical Showtime (disease incidence range: 50-88%; disease severity range: 17-51%) (Fig. 1). Conversely, the lowest levels of disease incidence and severity at the end of the growing seasons were observed in the cultivars Winter Red (disease incidence range: 4-42%; disease severity range: 0-13%) and Maryland Beauty (disease incidence range: 2-32%; disease severity range: 0-13%) (Fig. 1). Cultivars Winter Gold and Red Sprite had variable disease incidence levels compared to the best performing cultivars, with disease levels that were comparable to Winter Red and Maryland Beauty in 2021, but significantly higher compared to these two less susceptible cultivars in 2022 (Fig. 1). Cultivars Winter Gold, Red Sprite, and Chrysocarpa also had low levels of disease severity in both 2021 and 2022 (Fig. 1). AUDPC data for both incidence and severity reflected the same means separation as the final disease incidence and disease severity data, suggesting that the timing of symptom onset was not different between the cultivars tested (data not shown). Overall, these results suggest that Maryland Beauty and Winter Red have partial disease resistance to latent fruit rot caused by *D. ilicicola*.

Cultivar susceptibility screening – natural inoculum. While less consistent than the results from the artificially inoculated trials conducted in 2021 and 2022, disease data collected in 2021 from trials exposed to natural inoculum at two locations within a commercial nursery also revealed some significant differences in susceptibility to fruit rot between the winterberry cultivars assessed ($P < 0.05$). At the container yard location, the lowest disease incidence level was observed in Winter Red (disease incidence range: 0-8%), which outperformed Maryland Beauty (disease incidence range: 6-14%), Winter Gold (disease incidence range: 22-38%), Stoplight (disease incidence range: 32-42%), Red Sprite (disease incidence range: 18-28%), and Chrysocarpa (disease incidence: 37%) (Fig. 2A). However, no statistically significant differences in disease severity were observed at this location (Fig. 2B). Inversely, at the field location, cultivars Maryland Beauty (disease incidence range: 16-30%; disease severity range: 0-3%), Winter Red (disease incidence range: 8-36%; disease severity range: 0-6%), and Red Sprite (disease incidence range: 8-30%; disease severity range: 2-13%) had significantly lower levels of disease compared to Winter Gold (disease incidence range: 98-100%; disease severity range: 37-44%) and Chrysocarpa (disease incidence range: 86-100%; disease severity range: 16-24%) (Fig. 2). AUDPC data for both incidence and severity reflected the same means separation as the final disease incidence and disease severity

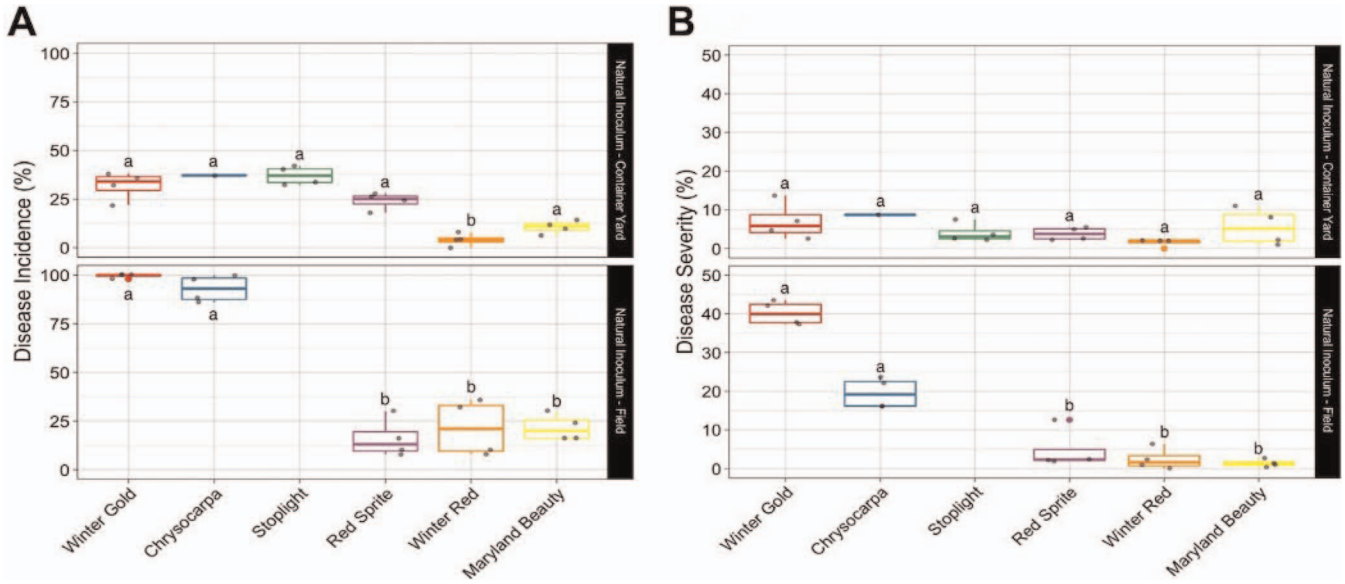

Fig. 2. Mean incidence (A) and severity (B) of latent fruit rot recorded at the end of the 2021 growing season from two outdoor trials conducted within a commercial nursery in Lake County, OH. The middle line in the boxplot represents the treatment median, while the upper and lower lines represent the upper and lower quartiles. Perpendicular lines connected to the upper and lower quartile lines indicate the range of the upper and lower 25% of datapoints. Datapoints separate from the boxplot indicate outliers. Means separation was performed using Tukey's HSD test (α=0.05). Different letters indicate significant differences in treatment mean.

data, suggesting that the timing of symptom onset was not different between the cultivars tested (data not shown).

It is also significant to note that within the commercial nursery, which relied upon natural inoculum, each plot location reflected a different production system. Differences in disease incidence and severity levels were observed among sites, suggesting that production practices may influence disease severity. The field plot had in-ground plants which received minimal management intervention between seasons. At this site, a maximum disease incidence of 100% and a maximum disease severity of 44% were observed. In the container yard plot, plants were maintained in pots and the surface of each pot was mulched. The maximum disease incidence observed at this site was 42% and the maximum disease severity was 14%. These results may reflect lower levels of inoculum in the container yard compared to the field, due to mummified fruit removal from branches and detritus removal from the surface of pots. Mulching of the surface of the pots may have also decreased disease severity by reducing airborne inoculum dispersal from wind and watersplash onto open flowers. While more targeted trials are needed to confirm the efficacy of these management strategies at reducing disease, *D. ilicicola* and other pathogens within the winterberry fruit rot complex are known to overwinter in mummified fruit and detritus (Lin et al. 2019b); therefore, removal of these sources of inoculum should reduce primary inoculum loads. Unfortunately, application of this method is not feasible in large-scale nursery field settings, and often, removal of mummified fruit is done exclusively by wildlife. Therefore, it may be advised for more susceptible cultivars, including Stoplight, Roberta Case, and Magical Showtime, to be maintained apart from large scale plantings and grown in areas which can be attended to with more attention. In terms of cultivar susceptibility, Maryland Beauty and Winter Red maintained the lowest levels of disease under all inoculation methods and production practices. This suggests that, while disease severity may vary by location, these two cultivars are promising candidates for resistance breeding efforts and the identification of metabolites associated with disease resistance.

Untargeted metabolomic analysis to identify differences in fruit chemistry. Notame clustering identified 2,807 clusters from within the 3486 total features within ESI − data, and 1,907 clusters from within the 2,606 total features within ESI + data. PCA comparison of the eight winterberry cultivar metabolomes revealed a visual separation between the less susceptible cultivars, Winter Red and Maryland Beauty on the top left, from the more susceptible cultivars Chrysocarpa, Magical Showtime, Red Sprite, Roberta Case, and Stoplight on the bottom right, in both positive and negative mode (Fig. 3). Notably, the cultivar Winter Gold also clustered with the two less susceptible cultivars, despite not showing a similarly less susceptible phenotype in the outdoor trials. This clustering phenomenon is likely due to the fact that Winter Gold is a sport of Winter Red, and therefore shares a similar metabolite profile. The majority of the observed separation by cultivar is accounted for by principal component (PC) 2, which explains 16.1% (ESI −) and 16% (ESI +) of the differences existing between samples. Observed separation by fruit phenological stage is accounted for by PC 1, which explains 20.6% (ESI −) and 22.3% (ESI +) of the differences between samples.

For further analysis, datasets for the three collection timepoints were separated and cultivars were divided into two groups based on their PC clustering by cultivar profile. PC clustering by cultivar group 1 consisted of the two less susceptible cultivars, Maryland Beauty and Winter Red,

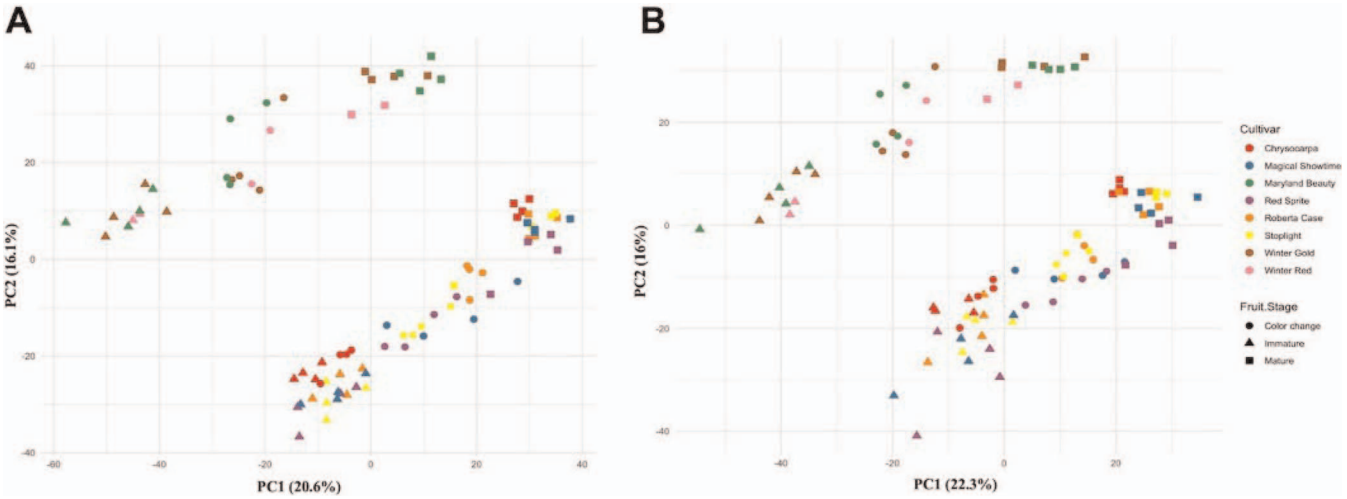

Fig. 3. Principal components analysis (PCA) of electrospray ionization (ESI) negative (A) and positive (B) LC-MS/MS data for features within the metabolome of eight winterberry cultivars (represented by color) at three fruit phenological stages of maturation (represented by shape). PCA scores were generated in MetaboAnalyst v. 5.0 using the statistical analysis [one factor] data import and processing function. Raw peak height data were normalized by median, natural log transformed and autoscaled (mean-centered and divided by the standard deviation of each variable.

along with Winter Gold; this group was labeled as the less susceptible group (denoted as "R"), because Maryland Beauty and Winter Red showed a less susceptible phenotype in the outdoor susceptibility screening trials. PC clustering by cultivar group 2 consisted of the cultivars Chrysocarpa, Magical Showtime, Red Sprite, Roberta Case, and Stoplight; this group was labeled as the more susceptible group (denoted as "S"), because these cultivars showed a more susceptible phenotype in the outdoor susceptibility screening trials. Univariate analysis combining t-test ($P < 0.001$) and fold-change (FC>150) parameters identified 48 features using ESI - mode data (Table 2A) and 41 features using ESI + mode data (Table 2B), which appear to be present at a higher abundance in the R group compared to the S group.

In the literature, antimicrobial compounds reported within *Ilex* include mainly triterpene saponins, phenolic acids, and the derivatives of these compounds. Some examples of antimicrobial triterpenoids reported in the literature to be present in the leaves and fruit of several *Ilex* species, including *I. verticillata* (L.) A. Gray, include ursolic acid, oleanolic acid, rotundic acid and peduncloside (Erdemoglu et al. 2009, Babalola and Shode 2013, Chen et al. 2011, Kothiyal et al. 2012, Harigushi et al. 1999). Additionally, *Ilex* fruits have been shown to accumulate cinnamic acid esters during the maturation process, with the presence of cinnamic acids confirmed in the fruits of 24 *Ilex* species, including *I. verticillata* (L.) A. Gray (Kothiyal et al. 2012, Sova 2012, Clifford and Ramirez-Martinez 1990, Alikaridis 1987). High levels of chlorogenic acid have also been observed in the leaves, bark, and fruit of many *Ilex* species, suggesting that these compounds may be conserved throughout the *Ilex* genus and may be present in the fruit of resistant *I. verticillata* (L.) A. Gray cultivars (Negrin et al. 2019, Alikaridis 1987, Prado Martin et al. 2013).

Within the eight *I. verticillata* (L.) A. Gray cultivars tested in these experiments, four features of interest, present at a higher abundance in the fruit of less susceptible compared to more susceptible cultivars, were annotated to a confidence level 1 utilizing the MoNA spectral database. Two of the identified features were from ESI − mode data (Table 2A) and two were from the ESI + mode data (Table 2B). ESI − mode compounds include hederasaponin B, and α-L-arabinopyranoside. ESI + mode compounds include R-kawain, and hydroxysydonic acid. All four compounds have reported bioactivity in the literature, but none are specifically proven to have antifungal properties. Hederasaponin B, also referred to as hederagenin B, is a triterpene saponin which has been isolated from *Hedera helix* L. (English ivy) and has shown antiviral and antioxidant activity (Song et al. 2014). A glycoside, α-L-arabinopyranoside, previously isolated from *Psidium guajava* (common guava) leaves, has shown antibacterial activity against the human pathogens *Salmonella enteritis* and *Bacillus cereus* (Mittal et al. 2010). Hydroxysydonic acid, initially isolated from the fungus, *Aspergillus sydowi*, is a sesquiterpenoid which has also shown moderate antibacterial activity against human pathogens, including methicillin-resistant strains of *Staphalococcus aureus* (Hamasaki et al. 1978, Li et al. 2018). Finally, R-kawain is a kavalactone, initially isolated from *Piper methysticum* (Kava); while this compound has not yet been associated with antimicrobial activity, its bioactivity in animal systems describes powerful glycation and lipid peroxidation end product inhibition, which may alter lipid metabolism within winterberry fruit and, consequently, cuticle integrity (Chompoo et al. 2011, Wang et al. 2021).

Thirty-four features of interest were annotated to a confidence level 3 based on a plausible accurate mass match using the HMDB. These compounds included the terpene lactones, ginkgolide A-C, cinnamic acid esters, 1-O-E-Cinnamoyl-(6-arabinosylglucose) and 1-O-Cinnamoyl-β-D-gentiobiose, stilbene glycoside, procyanidin dimer B7, terpene saponins, soyasaponin I-II, and the carbohydrate conjugate, tuliposide A. As stated previously, cinnamic acid

Table 2. Summary of electrospray ionization (ESI) negative mode (A) and positive mode (B) features exhibiting a fold change (FC) > 150 (α=0.001) in relative abundance in principal component (PC) group R (less susceptible) compared to group S (more susceptible). PC group R consisted of pooled data from cultivars Winter Red, Maryland Beauty, and Winter Gold. PC group S consisted of pooled data from cultivars Stoplight, Red Sprite, Roberta Case, Chrysocarpa, and Magical Showtime. Comparisons were made between R/S groups at three fruit phenological timepoints: immature fruit, fruit at color change, and mature fruit. Features were identified to three annotation confidence levels described by Blazenovic et al. (2018) and include level 1 (confident 2D structure identified using the MassBank of North America [MoNA] spectral database), level 3 (possible structure or class identified using the Human Metabolomic Database [HMDB]), and level 4 (unknown). When present within annotations, adducts are denoted following compound IDs within double parenthesis.

				Immature		Color change		Mature	
m/z	RT	Subclass	Compound ID	FC	*P*	FC	*P*	FC	*P*
A									
Annotation confidence level 1 - confident 2D structure (source: MoNA spectral database)									
733.4529	5.22	Terpene saponins	Hederasaponin B	1061	1.52×10^{-22}	-	-	-	-
911.5020	4.24	Triterpenoids	^{*Z}α-L-arabinopyroside	276	7.32×10^{-11}	701	7.85×10^{-15}	167	1.95×10^{-15}
Annotation confidence level 3 – possible structure or class (source: HMDB LC/MS mass database)									
441.1406	2.48	cinnamic acid esters	1-O-E-Cinnamoyl-(6-arabinosylglucose)	169	1.34×10^{-16}	-	-	-	-
441.1404	2.62	cinnamic acid esters	1-O-E-Cinnamoyl-(6-arabinosylglucose)	321	8.55×10^{-11}	561	2.04×10^{-10}	211	2.88×10^{-09}
555.1335	2.62	cinnamic acid esters	1-O-E-Cinnamoyl-(6-arabinosylglucose) ((+TFA))	883	3.02×10^{-15}	2020	3.99×10^{-20}	792	1.86×10^{-17}
471.1510	2.77	cinnamic acid esters	1-O-Cinnamoyl-β -D-gentiobiose	166	3.54×10^{-11}	-	-	-	-
439.1249	2.41	terpene lactones	Ginkgolide C	285	3.05×10^{-11}	171	1.87×10^{-15}	-	-
601.1783	2.44	terpene lactones	Ginkgolide C ((+FA))	506	1.44×10^{-15}	-	-	-	-
485.1303	2.49	terpene lactones	Ginkgolide C ((+FA))	382	7.46×10^{-13}	-	-	-	-
439.1247	2.59	terpene lactones	Ginkgolide C	279	3.86×10^{-14}	-	-	-	-
443.1198	2.60	terpene lactones	Ginkgolide C ((+Hac))	199	2.45×10^{-09}	519	1.19×10^{-11}	209	1.15×10^{-10}
439.1245	2.74	terpene lactones	Ginkgolide C	490	1.19×10^{-09}	617	1.41×10^{-09}	215	2.80×10^{-10}
439.1248	2.84	terpene lactones	Ginkgolide C	476	1.98×10^{-11}	919	1.34×10^{-14}	-	-
499.1467	2.91	terpene lactones	Ginkgolide C ((+Hac))	-	-	468	5.81×10^{-15}	240	1.24×10^{-14}
469.1354	2.79	terpene lactones	Ginkgolide B	1176	1.80×10^{-14}	1278	4.20×10^{-21}	236	6.25×10^{-17}
453.1406	2.80	terpene lactones	Ginkgolide A ((+FA))	-	-	232	4.71×10^{-12}	-	-
453.1406	2.94	terpene lactones	Ginkgolide A ((+FA))	-	-	301	7.90×10^{-16}	-	-
941.5128	4.17	terpene saponins	Soyasaponin I	1103	9.71×10^{-16}	1427	2.98×10^{-17}	473	2.02×10^{-13}
941.5129	4.26	Terpene saponins	Soyasaponin I	-	-	254	2.95×10^{-14}	-	-
957.5080	3.58	Terpene saponins	Soyasaponin II	-	-	358	5.42×10^{-11}	161	1.08×10^{-08}
Annotation confidence level 4 - unknown									
538.1417	2.45	-	-	7816	2.30×10^{-26}	1050	1.16×10^{-17}	-	-
1096.5581	3.49	-	-	356	4.59×10^{-06}	2459	1.07×10^{-22}	1735	1.11×10^{-18}
947.4787	3.68	-	-	577	2.33×10^{-17}	1022	3.26×10^{-16}	-	-
583.2873	3.08	-	-	-	-	974	1.01×10^{-18}	154	4.24×10^{-12}
1109.5320	3.50	-	-	-	-	799	5.20×10^{-17}	-	-
608.2087	0.30	-	-	394	6.47×10^{-12}	378	9.60×10^{-14}	798	1.48×10^{-16}
663.3062	3.17	-	-	714	2.31×10^{-14}	398	1.51×10^{-13}	770	1.95×10^{-15}
569.9932	2.91	-	-	337	8.09×10^{-14}	628	7.23×10^{-16}	741	3.86×10^{-19}
454.9750	2.90	-	-	-	-	254	4.00×10^{-13}	569	1.86×10^{-17}
281.1032	2.76	-	-	237	2.15×10^{-12}	405	4.83×10^{-14}	-	-
949.0011	4.01	-	-	271	3.25×10^{-11}	397	3.18×10^{-14}	239	9.54×10^{-14}
147.0452	2.29	-	-	363	3.99×10^{-13}	172	3.42×10^{-13}	-	-
617.2093	2.63	-	-	348	3.90×10^{-09}	205	1.61×10^{-10}	231	3.26×10^{-11}
604.1892	2.80	-	-	-	-	347	2.55×10^{-13}	262	1.35×10^{-13}
147.0449	2.91	-	-	175	5.22×10^{-11}	335	6.95×10^{-14}	-	-
472.1461	2.74	-	-	-	-	185	1.05×10^{-11}	310	5.04×10^{-12}
959.5139	3.67	-	-	-	-	289	3.81×10^{-14}	-	-

Table 2. Continued.

m/z	RT	Subclass	Compound ID	Immature FC	Immature *P*	Color change FC	Color change *P*	Mature FC	Mature *P*
926.5077	4.24	-	-	257	1.35×10^{-10}	198	2.48×10^{-10}	-	-
1046.5316	3.51	-	-	-	-	247	1.18×10^{-12}	-	-
197.0668	0.27	-	-	-	-	220	1.99×10^{-09}	-	-
617.2091	2.69	-	-	-	-	-	-	211	1.26×10^{-09}
427.0759	0.26	-	-	-	-	-	-	202	5.08×10^{-12}
427.1611	2.59	-	-	-	-	194	1.31×10^{-11}		
583.2828	3.52	-	-	-	-	179	6.98×10^{-11}	-	-
601.2147	3.14	-	-	170	2.29×10^{-10}		-	-	-
587.1990	2.81	-	-	-	-	160	2.80×10^{-10}	-	-
355.1036	3.01	-	-	-	-	156	6.65×10^{-12}	-	-
175.0249	2.45	-	-	153	3.20×10^{-16}	-	-	-	-
B									
Annotation confidence level 1 – confident 2D structure (source: MoNA spectral database)									
247.1325	2.32	Sesquiterpenoid	Hydroxysydonic acid	-	-	151	6.91×10^{-12}	-	-
213.0909	2.91	Kava-lactone	R-Kawain	-	-	335	3.39×10^{-19}	-	-
Annotation confidence level 3 – possible structure or class (source: HMDB LC/MS mass database)									
409.1488	2.55	Terpene lactones	Ginkgolide A	596	5.60×10^{-16}	1114	4.49×10^{-20}	-	-
409.149	2.77	Terpene lactones	Ginkgolide A	421	4.48×10^{-12}	667	4.59×10^{-14}	433	5.19×10^{-14}
425.1438	2.29	Terpene lactone	Ginkgolide B	-	-	472	1.11×10^{-14}	245	1.12×10^{-12}
425.1436	2.47	Terpene lactones	Ginkgolide B	184	4.63×10^{-11}	354	2.08×10^{-10}	248	1.01×10^{-9}
425.1437	2.62	Terpene lactones	Ginkgolide B	208	3.85×10^{-8}	397	2.99×10^{-9}	212	6.79×10^{-9}
425.1436	2.8	Terpene lactones	Ginkgolide B	493	1.62×10^{-13}	947	2.90×10^{-22}	162	1.28×10^{-14}
441.1387	2.62	Terpene lactones	Ginkgolide C	407	9.87×10^{-12}	1384	1.05×10^{-18}	309	5.29×10^{-14}
441.1388	2.75	Terpene lactones	Ginkgolide C	300	7.56×10^{-9}	645	1.70×10^{-11}	296	1.18×10^{-12}
443.1544	2.42	Cinnamic acid esters	1-O-E-Cinnamoyl-(6-arabinosylglucose)	401	7.12×10^{-15}	424	3.39×10^{-19}	-	-
443.1544	2.56	Cinnamic acid esters	1-O-E-Cinnamoyl-(6-arabinosylglucose)	156	1.96×10^{-10}	618	2.06×10^{-16}	287	9.04×10^{-14}
460.1812	2.8	Cinnamic acid esters	1-O-E-Cinnamoyl-(6-arabinosylglucose) ((+NH4))	177	2.08×10^{-12}	-	-	-	-
391.1382	2.84	Stilbene glycosides	Procyanidin dimer B7	-	-	246	2.67×10^{-15}	-	-
279.1072	3.48	Carbohydrates and carbohydrate conjugates	Tuliposide A	-	-	259	1.37×10^{-10}	-	-
279.1071	3.67	Carbohydrates and carbohydrate	Tuliposide A	237	4.99×10^{-15}	888	1.26×10^{-17}	242	9.24×10^{-11}
935.4974	3.68	Terpene saponin	Soyasaponin II ((+Na))	-	-	684	5.26×10^{-23}	-	-
Annotation confidence level 4 - unknown									
494.1863	2.45	-	-	759	1.52×10^{-13}	1801	2.83×10^{-21}	197	6.79×10^{-12}
309.1176	3.68	-	-	-	-	937	5.26×10^{-23}	397	1.28×10^{-13}
232.1047	2.94	-	-	219	1.01×10^{-08}	802	1.34×10^{-12}	568	1.13×10^{-11}
449.1417	2.78	-	-	604	1.41×10^{-16}	789	1.18×10^{-19}	414	6.22×10^{-18}
615.2505	2.15	-	-	675	1.35×10^{-17}	430	9.00×10^{-20}	332	1.11×10^{-15}
590.2438	2.64	-	-	624	1.73×10^{-13}	-	-	403	1.32×10^{-13}
919.502	4.26	-	-	223	6.58×10^{-18}	595	7.96×10^{-23}	234	1.71×10^{-13}
464.0763	2.91	-	-	-	-	-	-	498	1.76×10^{-17}
467.1883	2.33	-	-	185	1.02×10^{-13}	392	1.34×10^{-16}	-	-
444.1861	2.79	-	-	361	1.53×10^{-13}	-	-	-	-
476.1759	2.58	-	-	-	-	174	5.49×10^{-11}	346	3.30×10^{-14}
478.1914	2.48	-	-	189	3.13×10^{-09}	335	6.13×10^{-10}	-	-

Table 2. Continued.

m/z	RT	Subclass	Compound ID	Immature		Color change		Mature	
				FC	*P*	FC	*P*	FC	*P*
570.2292	2.48	-	-	-	-	274	4.36×10^{-15}	-	-
231.1014	3.26	-	-	-	-	268	8.23×10^{-13}	240	9.44×10^{-11}
461.1844	2.56	-	-	-	-	216	1.40×10^{-13}	-	-
188.0916	3.49	-	-	-	-	213	2.13×10^{-12}	-	-
451.1572	2.59	-	-	211	7.88×10^{-13}	155	2.48×10^{-12}	-	-
595.1988	2.7	-	-	-	-	181	3.78×10^{-12}	210	5.88×10^{-11}
838.3481	3	-	-	-	-	201	2.37×10^{-14}	-	-
560.2335	2.81	-	-	-	-	189	1.83×10^{-11}	173	1.78×10^{-10}
283.1172	2.63	-	-	-	-	188	1.03×10^{-11}	-	-
293.1014	2.63	-	-	183	1.54×10^{-12}	-	-	-	-
188.0916	4.24	-	-	-	-	178	1.77×10^{-11}	-	-
188.0916	3.68	-	-	-	-	176	5.20×10^{-13}	-	-

*z - (3β, 5ξ, 9ξ, 13ξ, 16β,17ξ, 23S)-20-Hydroxy-16,23:16,30-diepoxydammar-24-en-3-yl 6-deoxy-α-L-mannopyranosyl-(1->2)-[β-D-xylopyranosyl-(1->2)-β-D-glucopyranosyl-(1->3)]-α-L-arabinopyranoside

esters have been reported in *Ilex* leaf and fruit tissue and have shown inhibition toward human-pathogenic bacteria, viruses, and fungal pathogens (Negrin et al. 2019, Alikaridis 1987, Campa et al. 2008, Kothiyal et al. 2012). Similarly, ginkgolide A-C have shown inhibition toward select species of human pathogenic bacteria and yeasts (Mazzanti et al. 2000, Razna et al. 2020). Stilbene glycosides have been recognized for their antifungal abilities, with their potential use as scaffolds for the development of novel antifungal drugs being recognized by De Filippis et al. (2018). Notably, decreases in ginkgolide B-C, 1-O-cinnamoyl-(6-arabinosyl-glucose), and procyanidin dimer B7 have already been observed within *I. verticillata* (L.) A. Gray × *I. serrata* Thunb. 'Sparkleberry' fruit, with the natural disease resistance observed in immature winterberry fruit being attributed to the high abundance of these compounds, with the decrease in concentration of these compounds during fruit ripening speculated to contribute to late-season symptom onset (Emanuel, Cooperstone and Peduto Hand, personal communication). Therefore, increases in cinnamic acid esters, stilbene glycosides, and terpene lactones within the fruit of less susceptible cultivars strengthens the hypothesis that these compounds are contributing to resistance to fruit rot caused by *D. ilicicola*.

In conclusion, this study aimed to compare commercially available *I. verticillata* (L.) A. Gray cultivars for their degree of susceptibility to latent fruit rot, and to determine whether their susceptibility could be explained by differences in their metabolic profiles. Of the eight winterberry cultivars evaluated in these trials, two cultivars outperformed the other six under both natural and artificial inoculum conditions and in two distinctly different production systems by showing both lower disease incidence and severity. These two cultivars were Winter Red and Maryland Beauty. The ability to diversify the traits of *Ilex* using cross-species hybridization is a popular practice utilized by holly breeders to create unique hybrid cultivars, with selection traditionally based upon visual features and not biological fitness (Loizeau et al. 2005, Manen et al. 2010, Cuenoud et al. 2000). Given the lower susceptibility of Winter Red and Maryland Beauty to fruit rot, differences in host-resistance should be a new factor considered in winterberry breeding programs. Further research to identify the features of interest, outlined in Table 2, and test their bioactivity against winterberry fruit rot pathogens, including *D. ilicicola,* will reveal which compounds contribute to the observed differences in cultivar susceptibility. Long term, these studies could reveal novel antifungal compounds and identify markers for breeding more resistant winterberry cultivars.

Literature Cited

Alikaridis, F. 1987. Natural constituents of *Ilex* species. J. of Ethnopharmacol. 20:121–144.

Babalola, I. T. and F. O. Shode. 2013. Ubiquitous Ursolic Acid: a potentially pentacyclic triterpene natural product. Phytojournal 2(2):214–222.

Blazenovic, I., Kind, T., Ji, J., and O. Fiehn. 2018. Software tools and approaches for compound identification of LC-MS/MS data in metabolomics. Metabolites 8(2):31–54.

Campa, C., Rakotomalala, J. J. R., de Kochko, A., and S. Hamon. 2008. Chlorogenic acids: diversity in green beans of wild coffee species. Advances in Plant Physiology 10:421–437.

Chen, X. Q., Zan, K., Yang, J., Liu, X., Mao, Q., Zhang, L., Lai, M. X., and Q. Wang. 2011. Quantitative analysis of triterpenoids in different parts of *Ilex hainanensis*, *Ilex stewardii* and *Ilex pubescens* using HPLC-ELSD and HPLC-MS and antibacterial activity. Food Chemistry 126:1454–1459.

Chompoo, J., Upadhyay, A., Kishimoto, W., Makise, T., and S. Tawata. 2011. Advanced glycation end products inhibitors from Alpinia zerumbet rhizomes. Food Chemistry 129:709–715.

Clifford, M. N. and J. R. R. Ramirez-Martinez. 1990. Chlorogenic acids and purine alkaloids contents of mate (*Ilex paraguariensis* A. St.-Hil.) leaf and beverage. Food Chemistry 35:13–21.

Cuenoud, P., Del Pero Martinez, M. A., Loizeau, P. A., Spichiger, R., Andrews, S., and J. F. Manen. 2000. Molecular phylogeny and biogeography of the genus *Ilex* L. (Aquifoliaceae). Annals of Botany 85:111–122.

De Filippis, B., Ammazzalorso, A., Amoroso, R., and L. Giampietro. 2018. Stilbene derivatives as new perspective in antifungal medicinal chemistry. Drug Development Research 80:285–293.

Dengler, H. W. 1957. Handbook of Hollies. Journal of the American Horticultural Society, Inc. p. 1–7.

Deng, T., Nie, Z. L., Drew, B. T., Volis, S., Kin, C., Xiang, C. L., Zhang, J. W., Wang, Y. H., and H. Sun. 2015. Does the arcto-tertiary biogeographic hypothesis explain the disjunct distribution of northern hemisphere herbaceous plants? The case of Meehania (Lamiaceae). PLoS One. 10(2):85–91.

Emanuel, I. B., Laird, A. E., and F. Peduto Hand. 2023. Understanding the environmental and physiological factors affecting the biology of *Diaporthe ilicicola*, the fungus causing latent fruit rot in winterberry. Plant Disease First Look. doi: 10.1094/PDIS-11-22-2759-RE.

Erdemoglu, N., Iscan, G., Sener, B., and P. Palittapongarnpim. 2009. Antibacterial, antifungal, and antimycobacterial activity of *Ilex aquifolium* L. leaves. Pharmaceutical Biology 47(8):697–700.

Fiehn, O. 2006. Metabolite profiling in *Arabidopsis*. Methods Mol. Biol. 323:439–47. doi: 10.1385/1-59745-003-0:439.

Galle, F. C. 1997. Hollies: The Genus *Ilex*. Timber Press, Incorporated. 573 p.

Gargiullo, M. B., and E. W. Stiles. 1991. Chemical and nutritional differences between two bird-dispersed fruits: *Ilex opaca* Aiton and *Ilex verticillata* (L.) A. Gray. Journal of Chemical Ecology 17(6):1091–1106.

Hale, E. M. 1891. *Ilex cassine*, the aboriginal North American tea. Its history, distribution, and use among the native North American Indians. U.S. Department of Agriculture, Division of Botany. Bulletin No. 14. p. 7–12.

Klavus, A., Kokla, M., Noerman, S., Koistinen, V. M., Tuomainen, M., Zarei, I., Meuronen, T., Hakkinen, M. R., Rummukainen, S., Farizah Babu, A., Sallinen, T., Karkkaninen, O., Paananen, J., Broadhurst, D., Brunius, C., and K. Hanhineva. 2020. "Notame": workflow for non-targeted LC-MS metabolic profiling. Metabolites 10(4):135–170.

Kothiyal, S. K., Sati, S. C., Rawat, M. S. M., Sati, M. D., Semwal, D. K., Semwal, R. B., Sharma, A., Rawat, B., and A. Kumar. 2012. Chemical constituents and biological significance of the genus *Ilex* (*Aquifoliaceae*). The Natural Products Journal 2:212–224.

Li, W. T., Luo, D., Huang, J. N., Wang, L. L., Zhang, F. G., Xi, T., Liao, J. M., and Y. Y. Lu. 2017. Antibacterial constituents from Antarctic fungus, Aspergillus sydowii SP-1. Natural Product Research 32(6):662–667.

Li, H. Y., Yang, W. Q., Zhou, X. Z., Shao, F., Shen, T., Guan, H. Y., Zheng, J., and L. M. Zhang. 2022. Antibacterial and antifungal sesquiterpenoids: chemistry, resource and activity. Biomolecules 12(9):1271–1297.

Li, Y., Tao, W., Cheng, Z. H., and Z. T. Wang. 2006. New triterpene saponins and flavonol glycosides from the leaves of *Ilex cornuta*. Chinese Journal of Chemistry 24: 577–579.

Lin, S. and F. Peduto Hand. 2019a. Investigations on the timing of fruit infection by fungal pathogens causing fruit rot of deciduous holly. Plant Dis. 103:308–314.

Lin, S. and F. Peduto Hand. 2019b. Determining the sources of primary and secondary inoculum and seasonal inoculum dynamics of fungal pathogens causing fruit rot od deciduous holly. Plant Dis. 103:951–958.

Lin, S., Taylor, N. J., Peduto Hand, F. 2018. Identification and characterization of fungal pathogens causing fruit rot of deciduous holly. Plant Dis.. 102:2430–2445.

Loizeau, P. A., Barriera, G., Manen, J. F., and O. Broennimann. 2005. Towards an understanding of the distribution of *Ilex* L. (*Aquifoliaceae*) on a world-wide scale. Plant Diversity and Complexity Patterns 55:501–520.

Madden, L. V., and F. W. Nutter. 1995. Modeling crop losses at the field scale. Can. J. Plant Pathol. 17:124–137.

Manen, J. F., Barriera, G., Loizeau, P. A., and Y. Naciri. 2010. The history of extant *Ilex* species (*Aquirolaiaceae*): Evidence of hybridization within a Micocene radiation. Mol. Phylogen. and Evol. 57:961–977.

Mazzanti, G., Mascellino, M. T., Battinelli, L., Coluccia, D., Manganaro, M., and L. Saso. 2000. Antimicrobial investigation of semipurified fractions of *Ginko biloba* leaves. Journal of Ethnopharmacology 71:83–88.

De Mendiburu, F. and R. Simon. 2015. Agricolae – ten years of an open source statistical tool for experiments in breeding, agriculture and biology. Peer J PrePrints. doi:10.7287/peerj.preprints.1404v1.

Mittal, P., Gupta, V., Kaur, G., Garg, A. K., and S. Amarjeet. 2010. Phytochemistry and pharmacological activities of Psidium guajava: a review. International Journal of Pharmaceutical Sciences Research 1(9):9–19.

Murakami, A. N. N., Amboni, R. D. D. M. C., Prudencio, E. S., Amante, R. R., Fritzen-Freire, C. B., Boaventura, B. C. B., de Bona Munoz, I., dos Santos Branco, C., Salvador, M., and M. Maraschin. 2013. Concentration of biologically active compounds extracted from *Ilex paraguariansis* St. Hil. by nanofiltration. Food Chemistry 141:60–65.

NASS. 2019. Cut flowers: *Ilex* – sales, measured in $. https://quickstats.nass.usda.gov/#3216C4E-8135-34A-9DD8-7C54EB0E1CE6. Accessed May 1, 2023.

Negrin, A., Long, C., Motley, T. J., and E. J. Kennelley. 2019. LC-MS metabolomics and chemotaxonomy of caffeine-containing holly (*Ilex*) species and related taxa in the *Aquifoliaceae*. Journal of Agricultural and Food Chemistry 67:5687–5699.

Onesirosan, P., Arny, D., and R. D. Durbin. 1975. Increasing sporulation of Corynespora cassiicola. Mycopathologia 55(2):121–123.

Palo, R. T. and C. T. Robbins. 1991. Plant defenses against mammalian herbivory. CRC Press, Inc. p. 61–83.

Prado Martin, J. G., Porto, E., de Alencar, S. M., da Gloria, E. M., Correa, C. B., and I. S. Ribeiro Cabral. 2013. Antimicrobial activity of yerba mate (*Ilex paraguariensis* St. Hil.) against food pathogens. Rev Argent Microbiol. 45(2):93–98.

Razna, K., Sawinska, Z., Ivanisova, E., Vukovic, N., Terentijeva, M., Stricik, M., Kowalczewski, P. L., Hlavackova, L., Rovna, K., Ziarovska, J., and M. Kacaniova. 2020. Properties of Ginko biloba L.: antioxidant characterization, antimicrobial activities, and genomic micro-RNA based marker fingerprints. International Journal of Molecular Sciences 21:3087–3107.

Resch, J. 2020. Winterberry Workhorses. Holly Society Journal 38(1):12–14.

Salinas, J. and J. J. Sanchez-Serrano. 2006. Arabidopsis Protocols, 2nd Edition. Humana Press, Totowa, NJ. 496 p.

Smith Jr., J. P. 2019. Poisonous plants of the United States: a tabular summary. Botanical Studies. 67(14):1–17.

Song, J. Yeo, S. G., Hong, E. H., Lee, B. R., Kim, J. W., Kim, J., Jeong, H., Kwon, Y., Kim, H., Lee, S., Park, J. H., and H. J. Ko. 2014. Antiviral activity of hederasaponin B from *Hedera helix* against Enterovirus 71 subgenotypes C3 and C4a. Biomol. Ther. 22(1):41–46.

Sova, M. 2012. Antioxidant and antimicrobial activities of cinnamic acid derivatives. Bentham Science 12(8):1.

Thimmappa, R., Geisler, K., Louveau, T., O'Maille, P., and A. Osbourn. 2014. Triterpene biosynthesis in plants. Ann. Rev. Plant Biol. 65:225–257.

Vasconcelos, A. D., Dekker, R. F. H., Barbosa, A. M., and L. Paccola-Meirelles. 2001. Comparison of the laccases, molecular marker proteins and induction od pycnidia by three species of botrysphaeriaceous fungi. Mycoscience 42:543–548.

Wang, Y., Su, C., Zhang, B., Niu, Y., Ren, R., Zhao, X., Yang, L., Zhang, W., and X. Ma. 2021. Biological activity, hypatotoxicity, and structure-activity relationship of kavalactones and flavokavins, the two main bioactive components in Kava (Piper methysticum). Evidence-Based Complementary and Alternative Medicine 2021:1–14.

Weckwerth, W., Wenzel, K., and O. Fiehn. 2004. Process for the integrated extraction, identification and quantification of metabolites, proteins and RNA to reveal their co-regulation in biochemical networks. Proteomics 4:78–83.

Wu, Z. J., Ouyang, M. A., Wang, C. Z., Zhang, Z. K., and J. G. Shen. 2007. Anti-tobacco mosaic virus (TMV) triterpenoid saponins from the leaves of *Ilex oblonga*. Journal of Agricultural and Food Chemistry 55:1712–1717.

Yang, X., Yang, G., Li, W., Zhang, Y., and J. Wang, J. 2018. Therapeutic effects of *Ilex hainanensis* Merr. Extract of essential hypertension: a systematic review and meta-analysis of randomized controlled trials. Frontiers in Pharmacology 9(424):1–12.